

The existence of memory effect on hydrogen ordering in ice: The effect makes ice attractive

Masashi Arakawa,^{1,2,3} Hiroyuki Kagi,^{1,2} Jaime A. Fernandez-Baca,⁴
Bryan C. Chakoumakos,⁴ and Hiroshi Fukazawa²

Received 20 May 2011; revised 15 July 2011; accepted 15 July 2011; published 17 August 2011.

[1] The existence of ferroelectric ice XI with ordered hydrogen in space becomes of interest in astronomy and physical chemistry because of the strong electrostatic force. However, the influence was believed to be limited because it forms in a narrow temperature range. From neutron diffraction experiments, we found that small hydrogen-ordered domains exist at significantly higher temperature and the domains induce the growth of “bulk” ice XI. The small ordered domain is named “memory” of hydrogen ordered ice because it is the residual structure of ice XI. Since the memory exists up to at least 111 K, most of ices in the solar system are hydrogen ordered and may have ferroelectricity. The small hydrogen-ordered domains govern the cosmochemical properties of ice and evolution of icy grains in the universe.
Citation: Arakawa, M., H. Kagi, J. A. Fernandez-Baca, B. C. Chakoumakos, and H. Fukazawa (2011), The existence of memory effect on hydrogen ordering in ice: The effect makes ice attractive, *Geophys. Res. Lett.*, 38, L16101, doi:10.1029/2011GL048217.

1. Introduction

[2] The chemical properties of ice are governed by arrangement and dynamics of hydrogen atoms. Hydrogen atoms of normal ice (ice Ih) are disordered, having two crystallographically equivalent sites between two oxygen atoms [Bernal and Fowler, 1933; Pauling, 1935; Peterson and Levy, 1957]. In contrast, hydrogen atoms of ice XI, the hydrogen-ordered phase of ice Ih [Kawada, 1972; Tajima *et al.*, 1982], are located in one site, and the ordered hydrogen atoms make ice XI ferroelectric. Ice XI is only generated in impurity-doped ices. Structure of ice XI doped with KOD has been investigated by neutron diffraction experiments [Leadbetter *et al.*, 1985; Fukazawa *et al.*, 2005; Arakawa *et al.*, 2010]. In the doped ices, ice XI starts to nucleate at 60–65 K (57–62 K for H₂O ice) [Fukazawa *et al.*, 2006a], and it immediately disappears above the phase boundary (76 K for D₂O ice and 72 K for H₂O) between Ih and XI [Fukazawa *et al.*, 2006b].

[3] Lots of water ices exist as a crystalline phases in space [Kouchi *et al.*, 1994; Jewitt and Luu, 2004; Cook *et al.*,

2007]. Based on the numerous neutron diffraction studies for KOD-doped D₂O ice, Fukazawa *et al.* [2006a] proposed a hypothesis that ice XI exists in cold space environments. The nucleation and growth temperatures described above suggest that ferroelectric ice XI could exist on icy bodies or in interstellar molecular clouds where the temperatures are 57–62 K, but the temperature range seemed to be limited. For understanding the evolution of icy grains in the universe and astrochemical implication, the formation of ice XI doped with NaOD must be investigated because cosmic abundance of Na is 15 times as much as that of K. For precise understanding of nucleation and growth process of ice XI, we performed time-resolved neutron diffraction measurements of deuterium-substituted ice powders doped with 0.1 M NaOD. The relative intensity of the Bragg peak characteristic to ice XI in the neutron diffraction pattern of D₂O ice XI is about 10 times stronger than the corresponding peak in the X-ray diffraction pattern of hydrogenous ice XI. For this reason, neutron diffraction is the method of choice to study the nucleation and growth of ice XI.

2. Experimental Method

[4] We prepared NaOD-doped ice powder by rapid solidification of misted 0.1 M NaOD solution at 77 K. The mist passed through an atomizer with 400 μ m nozzle diameter into a cold stainless-steel vessel with a shallow pool of liquid nitrogen. By quickly freezing the solution, a substantial amount of NaOD is accommodated as an impurity in the ice lattice. Evaporation of all the liquid nitrogen left behind powdered ice on the bottom of the vessel. About 2 grams of the powdered ice was sealed in a vanadium can (10 mm diameter, 60 mm height) with helium gas to increase the thermal conductivity with the cold finger of a closed cycle helium cryostat. The neutron diffraction measurements were performed using the Wide Angle Neutron Diffractometer (WAND) [Katano *et al.*, 1998] installed in a research reactor, High Flux Isotope Reactor, at the Oak Ridge National Laboratory (ORNL). All the neutron diffraction patterns were collected using a wavelength of 1.476 Å with a step angle of 0.2°, and were saved every 5 min of collection time to observe the growth of ice XI with time.

3. Results and Discussion

[5] Typical neutron diffraction patterns of ice Ih and ice XI are respectively shown in Figures 1a and 1b. The major difference in diffraction patterns of ice XI and ice Ih is the presence of the isolated 131 Bragg peak in ice XI [e.g., Fukazawa *et al.*, 2005], while no peak occurs at that position for ice Ih. As shown in Figure 1b, the 131 Bragg peak orig-

¹Geochemical Research Center, Graduate School of Science, University of Tokyo, Tokyo, Japan.

²Quantum Beam Science Directorate, Japan Atomic Energy Agency, Tokai, Japan.

³Now at Quantum Chemistry Laboratory, Department of Chemistry, Faculty of Sciences, Kyushu University, Fukuoka, Japan.

⁴Neutron Scattering Science Division, Oak Ridge National Laboratory, Oak Ridge, Tennessee, USA.

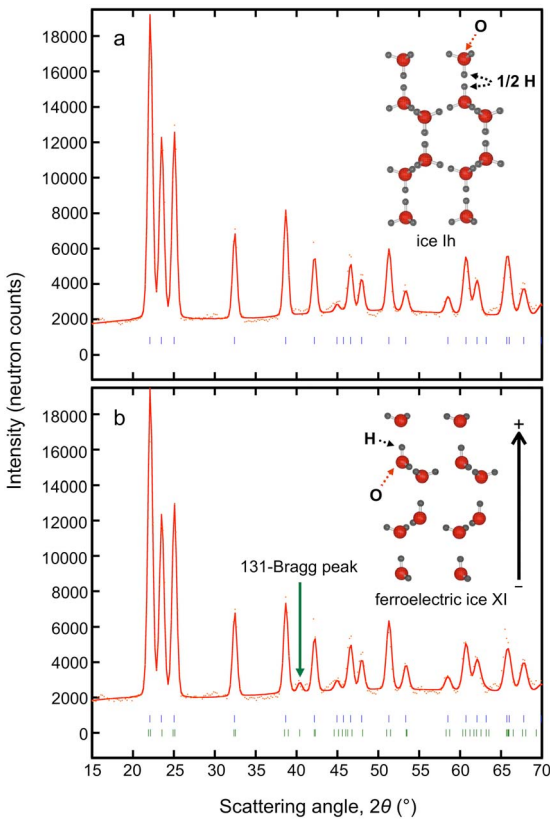


Figure 1. Typical neutron diffraction profiles of the 0.1 M NaOD-doped ice at sample temperature $T = 70$ K, which consists of (a) ice Ih, and (b) ice XI (14%) and ice Ih (86%). The dots mark the measured intensities. The solid line shows the calculated diffraction pattern using the best-fit parameters from Rietveld analysis. The peak positions calculated from the structure of ice Ih with hydrogen-disordered arrangement ($P6_3/mmc$) are shown by blue ticks below the diffraction patterns. The peak positions calculated from the structure of ice XI with the hydrogen-ordered arrangement ($Cmc2_1$) are shown by green ticks in Figure 1b. The 131 Bragg peak, which results from ice XI, was observed in Figure 1b at $2\theta = 40.28^\circ$. The insets show the crystal structure of ice Ih (Figure 1a) and ice XI (Figure 1b). The red and black circles respectively represent oxygen and hydrogen atoms.

inated from ice XI was observed at $2\theta = 40.28^\circ$, whereas no corresponding peak was observed for ice Ih shown in Figure 1a.

[6] Sample 1, which did not have the experience of changing into ice XI in the past, was mounted in a cryostat and cooled to 70 K. Neutron diffraction measurements were started when the temperature T reached 70 K. Figure 2a shows the diffraction profiles in the range of $2\theta = 39.48$ – 41.08° for the 131 Bragg peak, which results from the structure of ice XI. Yellow, white and blue regions show increasingly stronger intensities on the peak. The 131 Bragg peak was not observed, and the intensity in the range of $2\theta = 39.48$ – 41.08° did not increase with t , where t is the time passed since the measurements began. The results indicate that the formation of ice XI did not occur in Sample 1 at 70 K.

[7] We also measured the neutron diffraction profiles of Sample 2. The chemical composition and sample preparation

of Sample 2 were the same as those of Sample 1. The measurements were started when T reached 60 K. Obtained diffraction profiles are shown in Figure 2b. The 131 peak was not observed at $t = 0$, and grew with t until $t = 91.5$ hr. Because the peak is from the hydrogen ordered arrangement, the peak indicates the appearance of ice XI. We changed T from 60 K to 65 K at $t = 45.0$ hr and subsequently to 70 K at $t = 68.9$ hr, and the peak intensity increased more clearly until $t = 91.5$ hr. These results show that ice XI starts to grow at 60 K and it continuously grows at 65 and 70 K. When t reached 91.5 hr, the temperature of Sample 2 was

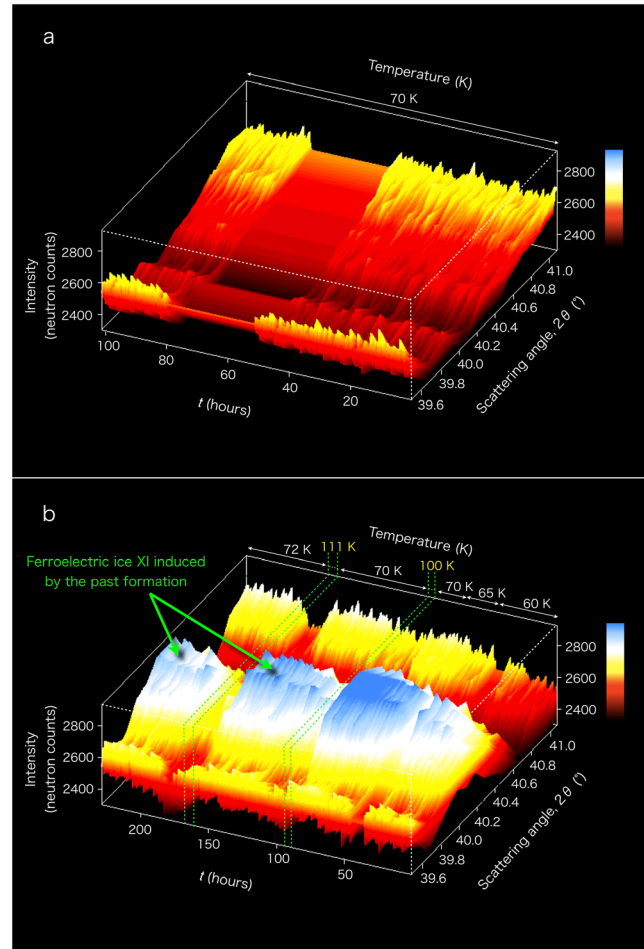


Figure 2. The 131 Bragg peak in the time-resolved neutron diffraction pattern for (a) Sample 1 and (b) Sample 2. Yellow, white and blue regions show increasingly strong intensities on the peak. The 131 Bragg peak from ice XI, which is forbidden in ice Ih, was not observed in Figure 2a. Ice XI is not formed at 70 K in the doped ice, which has not experienced changing into ice XI in the past. On the other hand, the Bragg peak appears at $2\theta = 40.28^\circ$ in Figure 2b and the intensity increases with time t until $t = 91.5$ hr. Ice XI starts to grow at 60 K and it continuously grows at 65 and 70 K. To transform ice XI back to ice Ih, the temperature of Sample 2 was raised above 76 K, the Ih-XI transition temperature, at $t = 91.5$ and 161.5 hr. After that, ice XI grows again when the back-transformed sample is kept at 70 K and 72 K. Data were not collected during $t = 51.11$ – 79.94 hr for Sample 1 and $t = 40.81$ – 48.52 hr for Sample 2.

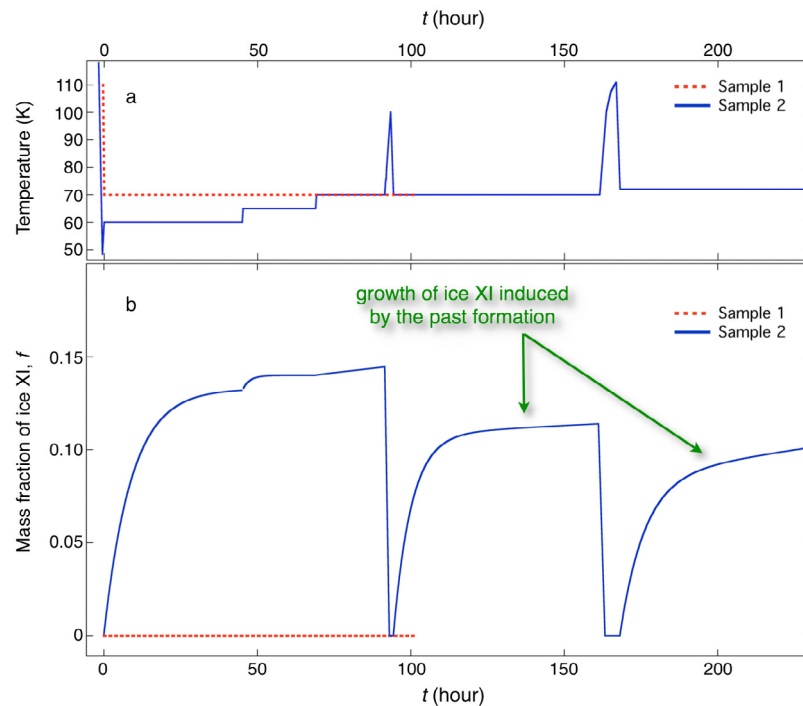


Figure 3. (a) Temperature history of the samples and (b) the mass fraction of ice XI to that of the doped ice (f) versus t .

raised to 100 K, above the Ih-XI transition temperature at 76 K, and the peak disappeared suddenly. Thus, ice XI vanished at 100 K.

[8] Then, Sample 2 was cooled to 70 K. The peak was observed again, and it became strong with t . The peak intensity is proportional to the mass; therefore, the result suggests that the mass of ice XI increased at 70 K. Enhancement of the growth of ice XI in addition to the nucleation below 65 K was already reported by Arakawa *et al.* [2010] using 0.013 M KOD-doped ices. However, nucleation of ice XI above 70 K has never been reported.

[9] The sample was warmed up to 111 K at $t = 161.5$ hr to transform it back to ice Ih. It was kept above the transition temperature for 6 hr. This is considered to be enough time to completely reverse the phase transition to ice Ih [Fukazawa *et al.*, 2006b]. The 131 Bragg peak disappeared, which indicates the sample was transformed to ordinary ice Ih again. After that, the sample was cooled to 72 K. The 131 Bragg peak appeared and the intensity increased with t again. Temperature histories of the samples are shown in Figure 3a.

[10] The phase transition from ice Ih to XI occurred in Sample 2 at 70 and 72 K whereas the transition did not occur in Sample 1 at 70 K. The only difference between Sample 1 and 2 is the prior experience of becoming ice XI. It is worthwhile to note that ice XI formed at higher temperatures than the nucleation temperature of ice XI at 65 K if the ice had the experience of becoming ice XI in the past. The mass fraction of ice XI to that of the doped ice (f) was estimated using Rietveld analysis. A two-phase model, which includes ice Ih and XI, were applied. Figure 3 schematically shows the mass fraction of ice XI (Figure 3b) with the temperature histories of the samples (Figure 3a). After Sample 2 was transformed back to ice Ih at $t = 91.5$ and 161.5 hr, the f value of Sample 2 increased again when the sample

was kept at 70 and 72 K. The growth of ice XI at 70 K was faster than that at 72 K. The results suggest that the driving force for the transformation to ice XI from Ih is larger at lower temperature.

[11] Previous studies showed that ice XI did not form at temperatures higher than 65 K. However, this study shows that the formation of ice XI at 70 and 72 K. This result suggests the presence of a template acting as the nuclei of ice XI. In general, a small metastable domain with a high ratio of the surface area to the volume can exist, even in a thermodynamically unstable condition. Thus, small domains with ordered hydrogen, which cannot be detected with neutron diffraction, exist above the boundary temperature between ice Ih and XI. It was reported that $5 \times 5 \times 5$ unit cells can even give broad diffraction peaks in the powder pattern [Neder and Proffen, 2008]. Therefore, the size of the small hydrogen-ordered domains which gave no observable diffraction pattern is considered to be smaller than several nanometers. The small ordered-domain is called “memory” of hydrogen ordered structure because of the residual structure of ice XI. We propose that the phenomenon reported here is named the “memory effect of hydrogen ordering”.

[12] The small ordered domains can exist because the local arrangement of hydrogen atoms is frozen below the glass transition temperature (in the region of 130–165 K [e.g., Velikov *et al.*, 2001]). Thus, the domains exist in bulk ice up to the glass transition temperature although the bulk properties of ice might be almost the same as ordinary ice. An inelastic neutron scattering study [Fukazawa *et al.*, 2003] also supports the existence of a small hydrogen-ordered domain. Small ice particles whose sizes are similar to the ordered domains can behave as hydrogen ordered domains. Therefore, small icy grains in space are hydrogen-ordered ice. Indeed, spectroscopic studies of thin ice film shows the hydrogen

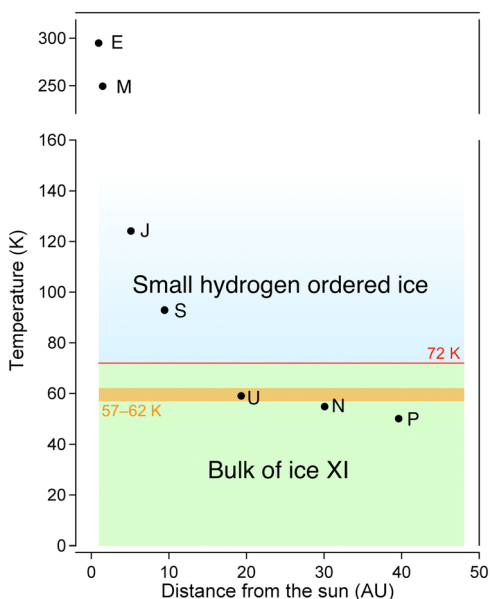


Figure 4. Area where the hydrogen ordered ice exists in our solar system. The blue area represents temperatures at which the small hydrogen ordered domains exist because of the “memory”. Bulk ice XI exists as a stable form below 72 K for H₂O ice (green area). The narrow orange area (57–62 K) shows the previously reported temperature range where the nucleation of ice XI occurs [Fukazawa *et al.*, 2006a]. Note that these temperatures are slightly lower than those reported in the present study on D₂O ices because of the H-D isotope effect. In this area, bulk of ice XI is formed without the “memory effect”. The E, M, J, S, U, N, and P respectively indicate Earth, Mars, Jupiter, Saturn, Uranus, Neptune, and Pluto.

ordered at temperatures higher than 76 K (up to about 150 K) [Su *et al.*, 1998; Wang *et al.*, 2005; Arakawa *et al.*, 2009]. Furthermore, molecular dynamics simulations also support the idea that small confined hydrogen-ordered structures should exist at higher temperatures [Mikami *et al.*, 2009]. Therefore, we conclude that the proposed small hydrogen-ordered domains exist in space at any temperatures below the glass transition temperature, if the ice has experienced temperatures below 72 K and becoming ferroelectric ice (Figure 4). Jupiter and Saturn are in the temperature range of the small hydrogen-ordered ice. Crystals in the Jovian and Saturnian region, however, had not experienced lower temperatures such as 57–62 K in the formation process of the solar system because ice crystal grains might be formed by the condensation of water vapor during the cooling of the solar nebula in the Jovian and Saturnian region.

[13] The OH⁻ ions, derived from the doped NaOD, substitute for H₂O sites in the ice, and increase the mobility of hydrogen atoms. Since the dopant acts as an accelerator for the transition, the observed “memory” effect occurs in other doped ices and natural ice with a small amount of defects. Strong electrostatic attractive force acts between the ferroelectric ices. Even if impact heating, formation of protostar, seasonal variation of planet, or the other astronomical processes raised the temperature of the ice, the small hydrogen-ordered domains could have remained and have influenced

planetary formation. The ferroelectric ice exists in the whole process of formation and evolution of protostar nebulae.

4. Conclusions

[14] Time-resolved neutron diffraction patterns of 0.1 M NaOD-doped ices were measured. The phase transition from ice Ih to XI occurred at higher temperatures than the nucleation temperature of ice XI at 65 K if the ice had the experience of becoming ice XI in the past. The results suggest that small hydrogen-ordered domains, which cannot be detected with neutron diffraction, exist above the boundary temperature between ice Ih and XI. This phenomenon enables hydrogen-ordered ferroelectric ice to remain up to 150 K. The ferroelectric ice could exist in the whole process of formation and evolution of protostar nebulae, and have played important roles in planetary formation and evolution of icy grains.

[15] **Acknowledgments.** This work was supported by the JAEA-ORNL part of the US-Japan Cooperative Program on Neutron Scattering. We thank C. Redmon and W. Zhou (ORNL) for assistance with the neutron powder diffraction experiments. This research was sponsored by the Division of Scientific User Facilities, Office of Basic Energy Sciences, U.S. Department of Energy. This study was financially supported by grants-in-aid for JSPS fellows (08J03621), for creative scientific research (19S0205), and for young scientists (18740342) from the Japan Society for Promotion of Science (JSPS) and the Global COE Programs for Chemistry Innovation and for Deep Earth Mineralogy.

References

- Arakawa, M., H. Kagi, and H. Fukazawa (2009), Laboratory measurements of infrared absorption spectra of hydrogen-ordered ice: A step to the exploration of ice XI in space, *Astrophys. J. Suppl. Ser.*, *184*, 361–365, doi:10.1088/0067-0049/184/2/361.
- Arakawa, M., H. Kagi, and H. Fukazawa (2010), Annealing effects on hydrogen ordering in KOD-doped ice observed using neutron diffraction, *J. Mol. Struct.*, *972*, 111–114, doi:10.1016/j.molstruc.2010.02.016.
- Bernal, J. D., and R. H. Fowler (1933), A theory of water and ionic solution, with particular reference to hydrogen and hydroxyl ions, *J. Chem. Phys.*, *1*, 515–548, doi:10.1063/1.1749327.
- Cook, J. C., S. J. Desch, T. L. Roush, C. A. Trujillo, and T. R. Geballe (2007), Near-infrared spectroscopy of Charon: Possible evidence for cryovolcanism of Kuiper belt objects, *Astrophys. J.*, *663*, 1406–1419, doi:10.1086/518222.
- Fukazawa, H., M. Oguro, S. M. Bennington, and S. Mae (2003), Phonon dispersion curves in KOD-doped ice observed by neutron scattering, *J. Chem. Phys.*, *118*, 1577–1579, doi:10.1063/1.1539846.
- Fukazawa, H., A. Hoshikawa, H. Yamauchi, Y. Yamaguchi, N. Igawa, and Y. Ishii (2005), Formation and growth of ice XI: A powder neutron diffraction study, *J. Cryst. Growth*, *282*, 251–259, doi:10.1016/j.jcrysgro.2005.04.105.
- Fukazawa, H., A. Hoshikawa, Y. Ishii, B. C. Chakoumakos, and J. A. Fernandez-Baca (2006a), Existence of ferroelectric ice in the Universe, *Astrophys. J.*, *652*, L57–L60, doi:10.1086/510017.
- Fukazawa, H., A. Hoshikawa, H. Yamauchi, Y. Yamaguchi, and Y. Ishii (2006b), Deuteron ordering in ice containing impurities: A neutron diffraction study, *Physica B*, *385–386*, 113–115, doi:10.1016/j.physb.2006.05.177.
- Jewitt, D. C., and J. Luu (2004), Crystalline water ice on the Kuiper belt object (50000) Quaoar, *Nature*, *432*, 731–733, doi:10.1038/nature03111.
- Katano, S., Y. Ishii, Y. Morii, H. R. Child, and J. A. Fernandez-Baca (1998), Upgrade of the wide-angle neutron diffractometer at the high-flux isotope reactor, *Physica B*, *241–243*, 198–200, doi:10.1016/S0921-4526(97)00550-4.
- Kawada, S. (1972), Dielectric dispersion and phase transition of KOD doped ice, *J. Phys. Soc. Jpn.*, *32*, 1442, doi:10.1143/JPSJ.32.1442.
- Kouchi, A., T. Yamamoto, T. Kozasa, and J. M. Greenberg (1994), Conditions for condensation and preservation of amorphous ice and crystallinity of astrophysical ices, *Astron. Astrophys.*, *290*, 1009–1018.
- Leadbetter, A. J., R. C. Ward, J. W. Clark, P. A. Tucker, T. Matsuo, and H. Suga (1985), The equilibrium low-temperature structure of ice, *J. Chem. Phys.*, *82*, 424–428, doi:10.1063/1.448763.

- Mikami, F., K. Matsuda, H. Kataura, and Y. Maniwa (2009), Dielectric properties of water inside single-walled carbon nanotubes, *ACS Nano*, *3*, 1279–1287, doi:10.1021/nm900221t.
- Neder, R. B., and T. Proffen (2008), *Diffuse Scattering and Defect Structure Simulations*, Oxford Univ. Press, New York, doi:10.1093/acprof:oso/9780199233694.001.0001.
- Pauling, L. (1935), The structure and entropy of ice and of other crystals with some randomness of atomic arrangement, *J. Am. Chem. Soc.*, *57*, 2680–2684, doi:10.1021/ja01315a102.
- Peterson, S. W., and H. A. Levy (1957), A single-crystal neutron diffraction study of heavy ice, *Acta Crystallogr.*, *10*, 70–76, doi:10.1107/S0365110X5700016X.
- Su, X., L. Lianos, Y. R. Shen, and G. A. Somorjai (1998), Surface-induced ferroelectric ice on Pt(111), *Phys. Rev. Lett.*, *80*, 1533–1536, doi:S0031-9007(97)05196-X.
- Tajima, Y., T. Matsuo, and T. Suga (1982), Phase transition in KOD-doped hexagonal ice, *Nature*, *299*, 810–812, doi:10.1038/299810a0.
- Velikov, V., S. Borick, and C. A. Angell (2001), The glass transition of water, based on hyperquenching experiments, *Science*, *294*, 2335–2338, doi:10.1126/science.1061757.
- Wang, H., R. C. Bell, M. J. Iedema, A. A. Tsekouras, and J. P. Cowin (2005), Pyroelectricity of water ice, *Astrophys. J.*, *620*, 1027–1032, doi:10.1086/427072.
-
- M. Arakawa, Quantum Chemistry Laboratory, Department of Chemistry, Faculty of Sciences, Kyushu University, 6-10-1 Hakozaki, Hikashi-ku, Fukuoka 812-8581, Japan. (arakawa@chem.kyushu-univ.jp)
- B. C. Chakoumakos and J. A. Fernandez-Baca, Neutron Scattering Science Division, Oak Ridge National Laboratory, PO Box 2008, Bldg. 7962, Oak Ridge, TN 37831-6393, USA. (chakoumakobc@ornl.gov; fernandezbja@ornl.gov)
- H. Fukazawa, Quantum Beam Science Directorate, Japan Atomic Energy Agency, 2-4 Shirane, Tokai, Ibaraki 319-1195, Japan. (fukazawa.hiroshi@jaea.go.jp)
- H. Kagi, Geochemical Research Center, Graduate School of Science, University of Tokyo, 7-3-1 Hongo, Bunkyo, Tokyo 113-0033, Japan. (kagi@eqchem.s.u-tokyo.ac.jp)